

# Numerical Modelling of the Mechanical Behaviour and Failure Modes of Timber Beams with Lapped Scarf Joints Using Wooden Dowels

Trong Tuan Tran<sup>1\*</sup>

<sup>1</sup> Faculty of Civil Engineering, Hanoi Architectural University, No. 129, Tran Phu Street, Ha Dong Ward, Hanoi 12100, Vietnam

\* Corresponding author, e-mail: [tuanttt@hau.edu.vn](mailto:tuanttt@hau.edu.vn)

Received: 19 March 2026, Accepted: 29 May 2026, Published online: 22 June 2026

## Abstract

This paper presents a numerical investigation of the mechanical behaviour and failure modes of a timber beam with a lapped scarf joint connected by wooden dowels. A finite element model was developed in Abaqus to analyse the structural response of the joint under bending loading. The timber material was modelled as an orthotropic material with nonlinear behaviour, incorporating an appropriate failure criterion to capture stiffness degradation and damage initiation in the structural components. In addition, different contact modelling assumptions between the elements of the joint were considered in order to evaluate their influence on the numerical results. The analysis shows that the numerical model is able to reproduce the global structural response of the beam with reasonable accuracy. However, significant differences in stress distribution and predicted failure modes are observed when different contact assumptions are adopted. The results highlight the important role of contact modelling in the numerical simulation of timber connections with wooden dowels and provide further insight for the development of more reliable finite element models for traditional timber joints.

## Keywords

timber structures, lapped scarf joint, wooden dowels, finite element modelling, contact modelling

## 1 Introduction

In recent years, timber structures have attracted increasing attention in the construction sector due to their low density, renewability, and reduced environmental impact. Along with the growing demand for sustainable structural solutions, mechanical timber connections using wooden dowels and wooden nails have been reconsidered as potential alternatives to metal fasteners in specific applications [1]. Within this context, lapped scarf joints with wooden dowels represent a traditional joining technique of practical relevance, particularly in the repair of deteriorated beam ends in historic timber structures [2].

From a design perspective, dowelled timber connections are commonly assessed on the basis of Johansen's yield theory and the provisions of Eurocode 5 [3, 4]. However, for traditional joints such as lapped scarf joints with inclined contact surfaces and wooden dowels, current design provisions remain limited. The behaviour of this type of connection depends simultaneously on the joint geometry, the number and arrangement of dowels, the interaction at the contact interface, and the tensile resistance of wood perpendicular

to the grain. As a result, simplified design formulae are often insufficient to describe the actual load-transfer mechanism and failure development of the joint [2].

Many previous studies have investigated dowelled timber connections through both experimental and numerical approaches. Experimental works have clarified the load-carrying capacity, stiffness, and failure mechanisms of timber joints [5, 6]. Recent studies have also investigated the use of densified wood dowels and wooden fasteners in timber joints and repair applications. Xu et al. [7] analysed the mechanical performance of timber-to-timber joints with densified wood dowels, while Conway et al. [8] examined the reinforcement of timber perpendicular to the grain using densified wooden dowels. Additional studies have explored the use of densified wooden nails and swelling dowels for timber assemblies and restoration works [9, 10]. These developments further demonstrate the growing interest in sustainable timber connection systems based on wood-based fasteners. Several authors have combined experiments with finite element modelling to study mortise-and-tenon joints, single-dowel

connections, and traditional scarf joints, showing that numerical simulation is an effective tool for analysing stress distribution, displacement, and damage concentration in such systems [11–14]. In addition, studies on perpendicular-to-grain tension, pull-out resistance of wooden pegs, and local failure mechanisms around dowel holes have contributed to a better understanding of brittle failure in mechanical timber joints [15–18]. For lapped scarf joints with wooden dowels in particular, Arciszewska-Kędzior et al. reported that repaired beams retained approximately 65% to 75% of the load-carrying capacity of the original member, while the elastic stiffness was not significantly reduced; the dominant experimentally observed failures were related to tension perpendicular to the grain in the vicinity of the dowel holes [2].

Studies published in *Periodica Polytechnica Civil Engineering* have also contributed to the numerical and experimental investigation of timber structures. Saad and Lengyel [19] developed a parametric finite element model to analyse the influence of knots and associated fibre deviations on the flexural behaviour of Norway spruce beams, highlighting the importance of local stress concentration and failure initiation in timber members under bending. Milić et al. [20] investigated a bolted steel–CLT composite connection through experimental push-out tests and finite element modelling, emphasizing the important role of nonlinear timber behaviour and contact phenomena in the force-transfer mechanism of timber-based connections. These studies further demonstrate the importance of advanced numerical modelling approaches for analysing stress redistribution, damage development, and contact-dependent mechanical behaviour in timber members and timber connections.

Furthermore, recent research has highlighted the important role of drying cracks and checks in aged timber members. Lengyel and Saad [21] showed that pre-existing checks may significantly modify stress distribution and initiate premature shear-related damage mechanisms in timber beams. This aspect is particularly relevant for timber repair applications, where existing defects and deterioration are often unavoidable.

In parallel with experimental research, several nonlinear constitutive models have been developed to describe the orthotropic, inelastic, and damage-sensitive behaviour of wood. Theoretical frameworks based on Hill's anisotropic yield criterion, Hoffman's failure criterion, and nonlinear orthotropic constitutive formulations have been widely used in the numerical analysis of timber structures [22–25]. More advanced studies have combined plasticity and

damage in order to improve the description of wood behaviour under complex stress states [26, 27]. On this basis, our most recent study developed an elasto-plastic-damage constitutive model for lapped scarf joints with wooden dowels and showed that the model could reproduce the load-displacement response and the experimentally observed failure location with satisfactory agreement [28].

Nevertheless, although material modelling has been increasingly refined, the role of contact modelling in numerical simulations of traditional timber joints has not yet been sufficiently clarified. In lapped scarf joints, the transfer of forces depends not only on the constitutive response of wood and dowels, but also on the mechanical interaction between the inclined contact surfaces and the dowel-hole interfaces. Different contact assumptions may therefore modify the stiffness of the joint, the redistribution of stresses, and the predicted damage pattern, even when the geometry, boundary conditions, and material parameters remain unchanged. This aspect has received far less attention than joint geometry or constitutive modelling, despite its direct influence on the predictive capability of finite element analyses.

The present study addresses this issue by investigating the numerical simulation of timber beams with lapped scarf joints connected by wooden dowels, with particular emphasis on interface interaction assumptions. Using the same experimental reference configuration and the same constitutive framework as in [28], the present study investigates a tie-contact representation and compares its response with the previously validated friction-contact model reported in [28]. The objective is not to propose a new material model, but to clarify how contact assumptions affect the global structural response, the stress-transfer mechanism, and the predicted failure pattern of the joint. The results provide a more explicit basis for evaluating the reliability of finite element models for traditional timber joints and show that contact modelling should be treated as a key modelling parameter rather than as a secondary numerical detail.

## 2 Experimental reference

This section briefly summarizes the experimental configuration used as the reference basis for the numerical study. Since the present paper focuses on numerical simulation, only the information required to define the joint geometry, material arrangement, support conditions, and loading scheme is presented. The reference test was adopted from the experimental work of Arciszewska-Kędzior et al. [2] and corresponds to the same configuration used in our previous numerical study [28].

**2.1 Test configuration**

The reference specimen was a timber beam with a lapped scarf joint connected by two wooden dowels. The beam was made of Norway spruce, whereas the dowels were made of English oak. Each dowel had a diameter of 24 mm. The beam had a total length of 6.0 m and a cross-section of  $0.20 \times 0.24$  m [2, 28].

The scarf joint had an overlap length of 1.38 m, and its centre was located 1.5 m from the nearest support, corresponding to approximately one quarter of the beam span [2, 28]. The geometry of the beam and the joint configuration are shown in Fig. 1.

**2.2 Loading setup**

The beam was tested under three-point bending, with a concentrated load applied at mid-span and two supports located at the beam ends [2, 28]. During the test, load and displacement were recorded, and the mid-span deflection was used to characterize the global mechanical response of the beam. The loading rate was 30 mm/min, and the test was continued until failure [2].

The same support arrangement and loading positions were adopted in the present finite element model to ensure consistency between the experimental reference and the numerical simulation. The experimental setup is presented in Fig. 2.

**2.3 Experimental results**

The reference experimental results consisted of three load–displacement curves obtained from timber beams

with lapped scarf joints connected by wooden dowels, corresponding to three test specimens. The curves show an approximately linear response in the initial stage, followed by a peak load and a post-peak softening phase associated with damage development in the joint region. For comparison with the numerical results, the experimental curves are presented in Fig. 3 [2, 28].

Regarding the observed failure behaviour, two characteristic mechanisms were reported by Arciszewska-Kędzior et al. [2]: tension failure perpendicular to the grain developing through the dowel-hole region and along pre-existing drying cracks, and a less extensive tension failure perpendicular to the grain at the bottom of the beam. These experimental observations are used as the reference basis for evaluating the predicted failure patterns of the numerical models.

**3 Numerical model**

The numerical model was developed on the basis of the reference experimental configuration presented in Section 2. The model geometry, boundary conditions, and material constitutive laws were adopted from our previous validated study [28]. The validated model reported in [28] was previously calibrated and validated against the experimental three-point bending tests conducted by Arciszewska-Kędzior et al. [2], including comparisons of the load–displacement response and the experimentally observed failure locations in the joint region.

Compared with the numerical model reported by Arciszewska-Kędzior et al. [2], the present model employs the same experimental reference configuration, including the general geometry of the lapped scarf joint, the three-point bending setup, and the softwood beam–hardwood dowel arrangement. However, the two modelling

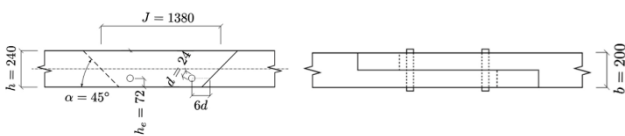


**Fig. 1** Geometry of the lapped scarf joint with wooden dowels (unit: mm) [2, 28]

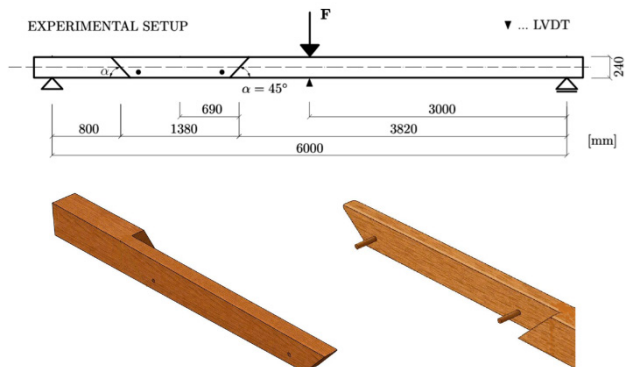


**Fig. 2** Experimental setup for the three-point bending test (unit: mm) [2, 28]

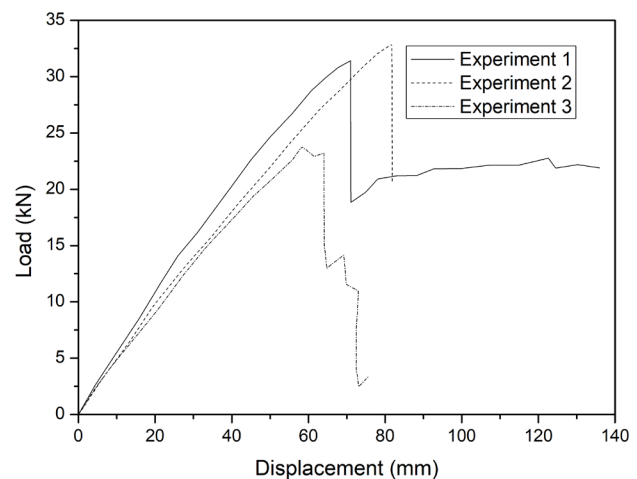


**Fig. 3** Load–displacement curves obtained from the experiments [2, 28]

approaches differ in several important aspects. The model presented in [2] was developed in ANSYS using SOLID95 elements, with Norway spruce and English oak represented as linear elastic orthotropic materials, and was primarily intended for investigating the influence of geometric parameters such as the number of dowels, joint length, and joint position. In contrast, the present model is based on the previously validated Abaqus framework developed in [28], in which the timber material response is described using a nonlinear elasto–plastic–damage formulation. Furthermore, the objective of the present study is not the optimization of joint geometry, but the investigation of contact modelling assumptions. Therefore, friction contact and tie contact are compared using the same geometry, boundary conditions, and material parameters in order to isolate the role of the contact formulation in the predicted structural response and failure pattern.

### 3.1 Finite element model

A three-dimensional finite element model of the timber beam with a lapped scarf joint connected by two wooden dowels was developed in Abaqus. The model reproduced the same beam geometry, joint dimensions, support arrangement, and loading position as those used in the reference experiment and in the previous numerical study [28]. The corresponding finite element model is shown in Fig. 4.

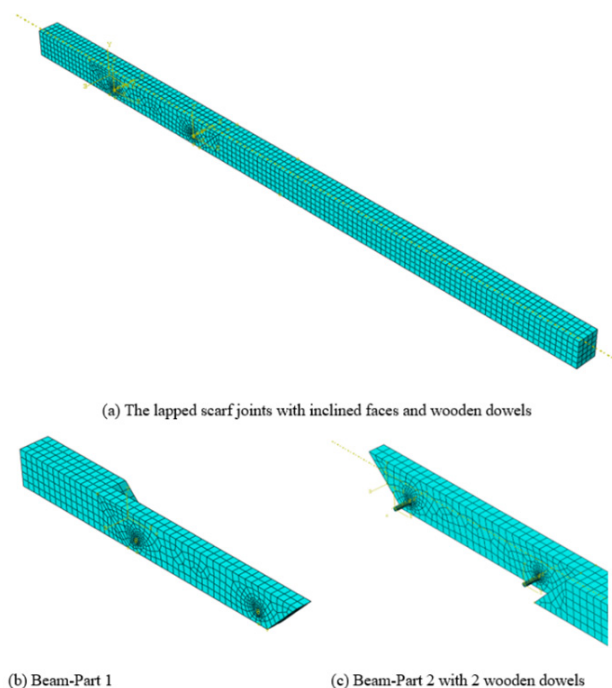


Fig. 4 Finite element model of the lapped scarf joint with wooden dowels [28]

Both the beam segments and the dowels were modelled using three-dimensional solid elements. The support conditions and loading scheme followed the three-point bending configuration described in Section 2. The mesh arrangement was directly inherited from the validated model reported in [28]; therefore, the mesh convergence procedure is not repeated here. This modelling strategy allows both the global load–displacement response and the local stress and damage development in the joint region to be captured.

### 3.2 Material model for wood

The material models used in the present study were also adopted from [28].

Norway spruce was used for the beam and was represented as a nonlinear orthotropic material combining elastic, plastic, and damage responses. Although wood is frequently idealized as a brittle orthotropic material, previous experimental and numerical studies have shown that timber may exhibit nonlinear inelastic behaviour before failure, particularly under compression parallel to the grain and under combined stress states. In the present model, the plastic component was introduced to represent irreversible deformation and stress redistribution prior to damage initiation, while the damage formulation was used to describe stiffness degradation and the development of failure in the timber members. English oak was used for the dowels and was modelled using the same constitutive framework with material parameters appropriate for hardwood [28]. This choice makes it possible to preserve consistency with the previously validated model while focusing the comparison on the contact conditions only. The anisotropic representation was considered necessary because timber exhibits strongly direction-dependent mechanical properties. This aspect is particularly important for lapped scarf joints, where the stress transfer around the dowel-hole region and the experimentally observed failure modes are closely related to tensile stresses perpendicular to the grain.

The principal mechanical properties adopted for Norway spruce and English oak are summarized in Tables 1 and 2, respectively [28]. Keeping the material parameters unchanged from the previous study ensures that any differences observed in the structural response, stress distribution, and predicted failure pattern can be attributed primarily to the adopted contact assumptions.

### 3.3 Contact modelling

The interfaces between the timber members and the wooden dowels were represented using contact constraints.

**Table 1** Mechanical properties of Norway spruce used for the beam model [28]

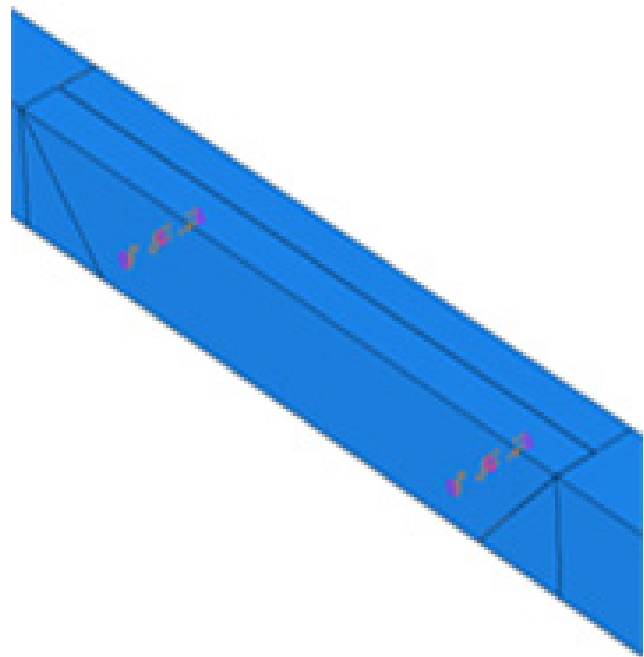
Property	Symbol	Value	Unit
Elastic properties			
Longitudinal modulus	$E_1$	13201	MPa
Radial modulus	$E_2$	763	MPa
Tangential modulus	$E_3$	279	MPa
Poisson's ratios	$\nu_{12}$	0.014	
	$\nu_{13}$	0.557	
	$\nu_{23}$	0.023	
Shear moduli	$G_{12}$	458	MPa
	$G_{13}$	554	-
	$G_{23}$	51.2	-
Plasticity parameters			
Hardening modulus	$Q$	100	MPa
Hardening coefficient	$b$	2.5	
Yield stress	$\sigma_e$	22	MPa
Compressive strengths	$f_{c,0}$	45	MPa
	$f_{c,90}$	4.5	-
Tensile strengths	$f_{t,0}$	22	MPa
	$f_{t,90}$	2.9	-
Shear strength	$f_{v,12} = f_{v,13}$	1.75	MPa
Damage parameters			
Damage threshold	$S$	0.00375	
Damage exponent	$s$	1.4	

**Table 2** Mechanical properties of English oak used for the dowel model [28]

Elastic properties	Symbol	Value	Unit
Longitudinal modulus	$E_1$	11178	MPa
Radial modulus	$E_2$	1028	MPa
Tangential modulus	$E_3$	2046	MPa
Poisson's ratios	$\nu_{12}$	0.064	
	$\nu_{13}$	0.37	
	$\nu_{23}$	0.033	
Shear moduli	$G_{12}$	1100	MPa
	$G_{13}$	234	-
	$G_{23}$	1041	-

In the previously validated model reported in [28], Coulomb friction contact was adopted, allowing relative displacement between the contacting surfaces. In the present model, tie-contact constraints were employed, meaning that the connected interfaces were assumed to move together without relative displacement. A schematic illustration of the tie-contact representation adopted in the present numerical model is shown in Fig. 5.

The main objective of the present study is to evaluate the influence of contact modelling on the behaviour

**Fig. 5** Schematic illustration of the tie-contact representation adopted between the timber beam segments and the wooden dowels in the present numerical model

of lapped scarf joints connected by wooden dowels. The present tie-contact model is therefore compared with the previously validated friction-contact model reported in [28], while preserving the same geometry, boundary conditions, and material parameters.

In the friction-contact model reported in [28], load transfer occurred through local contact interaction combined with friction, which can better represent the actual mechanical interaction between the inclined scarf surfaces and the dowel-hole interfaces. In contrast, the tie-contact formulation adopted in the present study assumes perfectly bonded interfaces without relative displacement. Compared with friction contact, this assumption introduces a stronger kinematic constraint and may therefore alter the load-transfer mechanism, stress redistribution, and predicted damage evolution in the joint.

The comparison between the previously validated friction-contact model and the present tie-contact model makes it possible to evaluate the sensitivity of the numerical results to the adopted interface assumption.

## 4 Results

### 4.1 Structural response

The overall response of the timber beam was evaluated through the mid-span load-displacement relationship. Fig. 6 presents the three experimental curves together

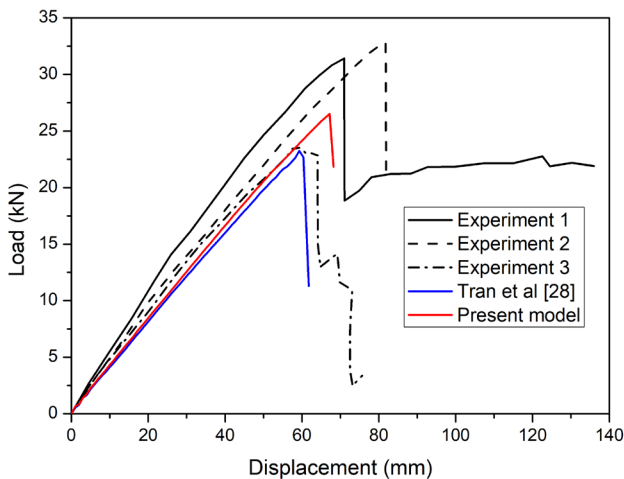


**Fig. 6** Load–displacement curves obtained from the experiments, the previous friction-contact model [28], and the present tie-contact model with the numerical result obtained from the previous friction-contact model [28] and the result obtained from the present tie-contact model. This comparison enables a direct assessment of the capability of the new numerical model to reproduce the global behaviour of the structural member.

The curves indicate that both the previous model [28] and the present model reproduce the initial stiffness of the structural member reasonably well in the near-linear stage. The response predicted by the present model follows the experimental curves more closely within the small-to-moderate displacement range, indicating that the finite element model retains a satisfactory ability to capture the initial elastic response of the jointed beam. Compared with the model reported in the previous study [28], the present model also shows a trend that is closer to the experimental results during the loading stage, particularly in terms of the initial slope and the evolution of load before the peak is reached.

However, noticeable differences appear as the structural member approaches the maximum load. The three experimental specimens exhibit a certain scatter in both the peak load and the corresponding displacement, reflecting the inherent heterogeneity of timber as well as the influence of natural defects in the joint region. Within this context, the present model predicts a peak load that lies within a reasonable range relative to the experimental results, although it remains lower than that of the specimen with the highest load-carrying capacity. This suggests that the present model provides a relatively conservative prediction of the ultimate resistance of the jointed beam.

After the peak load is reached, the experimental curves show a pronounced drop in load, associated with the initiation and development of damage in the joint region. The present model is also able to reproduce this general

descending trend, although the magnitude of the drop and the shape of the post-peak branch do not fully coincide with those of each individual test specimen. This discrepancy is acceptable, since the post-peak response of timber elements is strongly influenced by local cracking mechanisms, contact conditions, and the progression of damage around the dowel holes, all of which are highly sensitive to modelling assumptions.

Overall, the results shown in Fig. 6 demonstrate that the present model is capable of describing the global structural response of the timber beam with a lapped scarf joint connected by wooden dowels with reasonable accuracy, especially in the pre-peak stage. At the same time, the difference between the present model and the results reported in [28] indicates that modifying the modelling assumptions, particularly those related to contact interaction, has a significant influence on the load-displacement response of the structural member. This provides the basis for a more detailed analysis of stress distribution and failure modes in the following sections.

#### 4.2 Stress distribution

To clarify the load-transfer mechanism in the lapped scarf joint with wooden dowels, the equivalent stress distribution of the present tie-contact model was examined at three characteristic displacement levels, namely  $v = 10$  mm,  $v = 30$  mm, and  $v = 60$  mm. Although equivalent stress is not a failure criterion for orthotropic wood in a strict constitutive sense, it is used here as a convenient scalar indicator to visualize the development and redistribution of the stress field in the joint region. Fig. 7 presents the stress distribution in the two timber beam segments, whereas Fig. 8 shows the stress distribution in the two wooden dowels. These results are used to analyse the stress development in the present model and to compare it with the friction-contact results reported in the previous study [28].

Fig. 7 shows that, as the displacement increases from 10 mm to 60 mm, the stress field in the timber beam segments develops markedly in the vicinity of the joint. At the initial stage ( $v = 10$  mm), the stress remains relatively localized around the inclined contact surfaces and the dowel-hole region. When the displacement increases to 30 mm, the high-stress zone expands along the load-transfer path between the two beam segments. At  $v = 60$  mm, the stress field becomes more pronounced and spreads further into the beam segment adjacent to the joint, indicating that the tie-contact assumption promotes a more continuous transfer of forces through the connected timber members.

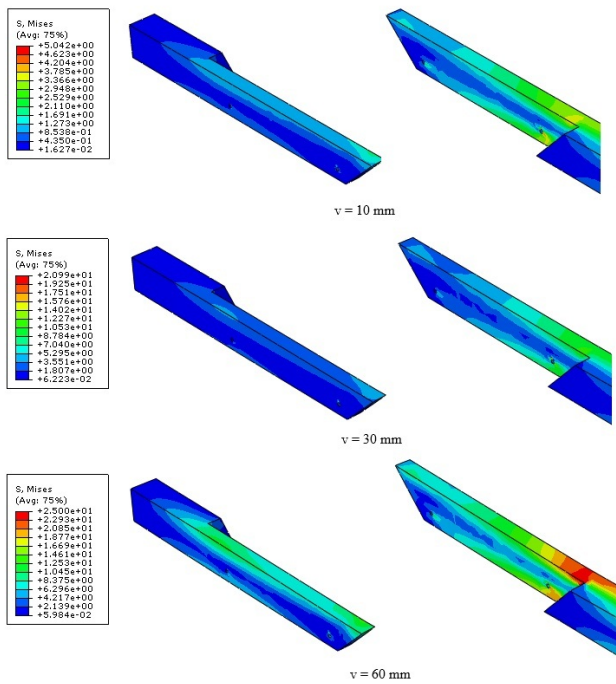


Fig. 7 Von Mises stress distribution in the two timber beam segments of the present tie-contact model at different displacement levels

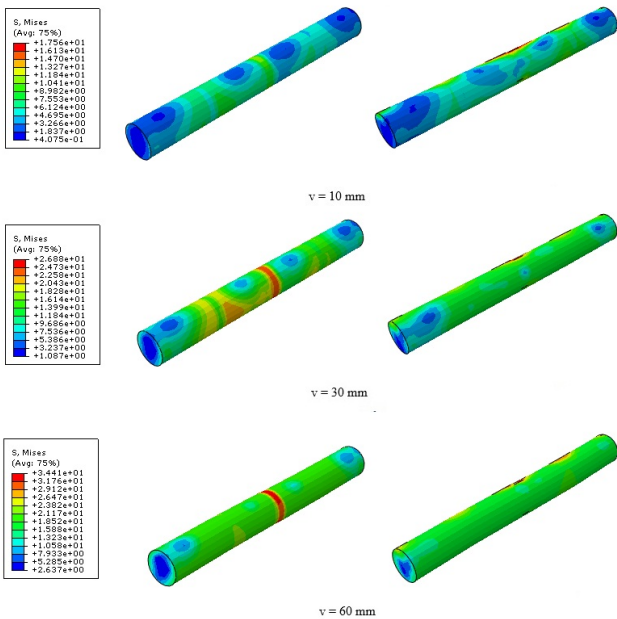


Fig. 8 Von Mises stress distribution in the two wooden dowels of the present tie-contact model at different displacement levels

Compared with the friction-contact results reported in [28], the stress field in the present model shows a broader and more continuous development within the beam segments, rather than remaining mainly concentrated around the principal contact zones. This suggests that the adopted contact assumption affects not only the intensity of local stress concentration but also the extent of stress redistribution in the timber beam near the scarf connection.

For the wooden dowels, Fig. 8 shows that stress appears from the early stage of loading, confirming their direct contribution to the force-transfer mechanism of the joint. At  $v = 10$  mm, the stress is mainly concentrated in the regions in contact with the hole wall. As the displacement increases to 30 mm, the stress level rises significantly and becomes more clearly distributed along the dowel length. At  $v = 60$  mm, both dowels are fully mobilized, with high-stress regions extending over a considerable portion of their length. This result indicates that, in the tie-contact model, the wooden dowels participate more actively in the overall mechanical response of the joint.

By comparison with the friction-contact model in [28], the present tie-contact model leads to a more continuous stress distribution along both dowels, whereas the previous model exhibited a more localized load-transfer mechanism. This difference reflects the stronger kinematic constraint introduced by the tie-contact assumption and its influence on how the dowels interact mechanically with the surrounding timber.

Overall, the results shown in Figs. 7 and 8 indicate that the tie-contact model creates a tighter interaction between the timber beam segments and the wooden dowels, thereby modifying the stress field throughout the joint region. These equivalent stress contours should be interpreted primarily as qualitative indicators of stress redistribution. The implication of this altered stress-transfer mechanism for the predicted failure pattern of the beam is discussed in the following section.

### 4.3 Failure modes

The failure modes predicted by the numerical model were analysed through the damaged zones appearing in the beam as the response approached failure. Fig. 9 presents the Abaqus predictions for the two contact assumptions, where the image on the left corresponds to the friction-contact model, while the image on the right corresponds to the tie-contact model.

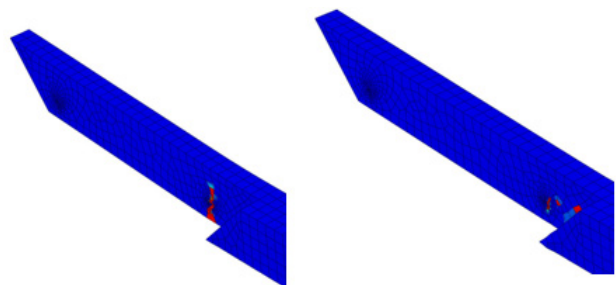


Fig. 9 Comparison of predicted failure modes in Abaqus for the friction-contact model (left) and the tie-contact model (right)

The simulation results show that the two contact assumptions lead to distinctly different failure patterns in the joint region. In the friction-contact case, the damaged zone is clearly concentrated in the beam segment near the dowel-hole region and develops almost perpendicular to the wood grain. This failure pattern is consistent with Failure 1 observed in the experiments, namely a tension failure perpendicular to the grain occurring in the beam body and propagating through the dowel-hole region and along pre-existing drying cracks. This indicates that the friction-contact model is able to reproduce reasonably well the localized failure mechanism around the dowel hole, which is one of the characteristic failure modes reported in the experimental study [2].

In contrast, in the tie-contact case, the damaged zone is no longer mainly concentrated around the dowel hole, but instead shifts towards the bottom of the beam in the vicinity of the joint region. This pattern is more consistent with Failure 2 observed experimentally, namely a less extensive tension failure perpendicular to the grain occurring at the bottom of the beam. Compared with the friction-contact model, the tie-contact assumption imposes a higher degree of constraint between the contacting surfaces, thereby altering the load-transfer mechanism within the joint and leading to a different location of damage initiation.

The difference between the two numerical models is consistent with the stress distribution results discussed in the previous section. Whereas the friction-contact model produces a more localized stress concentration around the dowel-hole region and the contact interface, the tie-contact model leads to a more continuous development of the stress field within the beam near the joint, particularly towards the lower part of the beam. This change in the stress field provides a clear mechanical explanation for the difference in the predicted failure modes.

Overall, changing the contact assumption affects not only the load-displacement response and the stress distribution, but also directly alters the predicted failure mechanism of

the structural member. The results shown in Fig. 9 indicate that the friction-contact model is closer to Failure 1 observed experimentally, whereas the tie-contact model gives a failure pattern that is closer to Failure 2. This confirms that the contact model is a decisive parameter in the numerical simulation of lapped scarf joints connected by wooden dowels.

#### 4.4 Discussion

To support the qualitative comparison with quantitative evidence, the main response parameters obtained from the experiment, the previous numerical model [28], and the present numerical model are compared in Table 3. The comparison includes the initial stiffness, the peak load, the displacement at peak load, and the dominant failure pattern.

Table 3 shows that the present model is closer to the experimental response than the previous model in terms of initial stiffness, peak load, and displacement at peak load. This indicates that the modification of the contact assumption improves not only the apparent agreement of the load-displacement curve, but also the quantitative prediction of the global structural response.

From a mechanical point of view, this result is significant because the geometry, boundary conditions, and material constitutive laws were kept unchanged with respect to the previous model [28]. The main difference between the two simulations lies in the contact formulation. Therefore, the improvement observed in Table 3 can be attributed primarily to the altered representation of the interaction between the inclined contact surfaces and the dowel-hole interfaces. This confirms that, for traditional timber joints of this type, the contact model is not a secondary numerical detail, but a parameter that directly affects the predictive capability of the finite element model.

The influence of the contact assumption becomes even clearer when the stress development and damage patterns are considered together. In the friction-contact model, the load-transfer mechanism remains more localized around the dowel-hole region and the principal contact surfaces.

**Table 3** Quantitative comparison between the experimental response, the previous numerical model,

Parameter	Experimental response	Previous model [28]	Present model
Initial stiffness, $K$ (kN/mm)	0.46	0.42	0.44
Peak load, $P_{max}$ (kN)	29.3	23.0	26.0
Mid-span displacement at peak load, $u_{p_{max}}$ (mm)	66	59	65
Dominant failure pattern	Tension perpendicular to the grain in the dowel-hole region; minor bottom tensile failure	Damage concentrated mainly around the dowel-hole region	Damage shifted towards the lower beam region near the joint; pattern closer to the secondary experimental failure mode

As a result, the stress field develops mainly in the vicinity of the interfaces, and the predicted damage tends to remain concentrated around the dowel-hole zone. In contrast, in the tie-contact model, the connected surfaces are constrained more strongly, which promotes a more continuous transfer of forces through the joint region. This leads to a broader stress development in the beam near the scarf connection and a clearer mobilization of the wooden dowels in the load-transfer process.

The difference in the internal force-transfer mechanism is reflected in the predicted failure pattern. The previous model is more consistent with the first experimentally observed failure mode, namely tension perpendicular to the grain developing through the dowel-hole region and along pre-existing drying cracks. By contrast, the present model predicts a damage zone that shifts towards the lower part of the beam near the joint and is therefore closer to the secondary experimental failure mode, namely a less extensive tensile failure perpendicular to the grain at the beam bottom. This comparison suggests that changing the contact assumption does not merely modify the numerical response in a local sense, but can substantially alter the predicted structural failure mechanism.

These findings have an important implication for the numerical simulation of timber joints. In many finite element studies, considerable attention is usually given to the constitutive model of wood and to the identification of material parameters, whereas the contact conditions are often introduced in a simplified manner. The present results show that such simplification may strongly influence both the global response and the predicted damage evolution. For this reason, the contact formulation should be regarded as a key modelling parameter, with a level of importance comparable to that of the constitutive law itself.

At the same time, the present conclusions should be interpreted within the scope of the study. The comparison was carried out for one joint geometry, one dowel arrangement, and one loading configuration under three-point bending. In addition, the quantitative values summarized in Table 3 are approximate values estimated from the plotted curves and are mainly intended to support the comparative discussion. A more detailed assessment based on the original experimental and numerical datasets would allow a more rigorous parameter-by-parameter validation. Nevertheless, even at this level, the results clearly demonstrate that the choice of contact assumption has a direct and non-negligible influence on the predicted behaviour of lapped scarf joints connected by wooden dowels.

Overall, the present study shows that the transition from the previous contact representation to the current one leads to a more accurate prediction of the global response and to a failure pattern that is closer to one of the experimentally observed damage scenarios. This reinforces the conclusion that contact modelling should be treated as a decisive modelling choice in finite element analyses of traditional timber joints, rather than as a purely technical implementation detail.

Nevertheless, it should also be noted that pre-existing drying cracks were not explicitly represented in the present numerical model. This assumption was intentionally retained in order to isolate the influence of the contact formulation while preserving consistency with the previously validated modelling framework [28]. Previous studies have shown that checks and cracks may significantly affect local stress concentrations and failure development in aged timber members [21]. Therefore, the interaction between contact behaviour and pre-existing drying cracks in lapped scarf joints should be further investigated in future studies.

## 5 Conclusions

This paper has presented a numerical study on the mechanical behaviour and failure modes of timber beams with lapped scarf joints connected by wooden dowels. Based on the results obtained, the following conclusions can be drawn:

- The present finite element model is able to reproduce the global load-displacement response of the jointed timber beam with reasonable accuracy, particularly in the pre-peak stage.
- The contact assumption has a pronounced influence on the predicted mechanical response of the joint, affecting not only the global structural behaviour but also the local stress distribution in both the timber beam and the wooden dowels.
- In the friction-contact model, the stress field tends to remain more localized around the dowel-hole region and the principal contact surfaces, leading to a failure pattern that is consistent with Failure 1 observed experimentally.
- In the tie-contact model, the stress field develops more continuously within the joint region and the lower part of the beam, while the dowels are more strongly mobilized in the load-transfer process. This results in a predicted failure mode that is closer to Failure 2 observed in the experiments.
- The quantitative comparison indicates that the present tie-contact model provides a closer approximation of the global structural response, particularly in

terms of initial stiffness, peak load, and displacement at peak load. However, the two contact representations reproduce different experimentally observed damage scenarios. The previously validated friction-contact model [28] is more consistent with the localized damage mechanism around the dowel-hole region, whereas the present tie-contact model gives a failure pattern closer to the secondary experimentally observed failure mode in the lower beam region.

- These findings show that no single contact representation should be regarded as universally superior for all modelling objectives. If the main objective is to reproduce the global load–displacement response, the tie-contact formulation may provide a better

approximation for the investigated configuration. If the objective is to capture localized damage around the dowel-hole region, the friction-contact formulation remains relevant. Therefore, the selection of contact modelling strategy should depend on the specific structural response or damage mechanism of interest for the investigated joint configuration.

### Acknowledgement

The author wishes to express sincere gratitude to Mr. Ngoc Tien Dao of Hanoi Architectural University for his valuable contributions and insightful suggestions, which have been instrumental in enhancing the quality of this research work.

### References

- [1] Sotayo, A., Bradley, D., Bather, M., Sareh, P., Oudjene, M., ..., Guan, Z. "Review of state of the art of dowel laminated timber members and densified wood materials as sustainable engineered wood products for construction and building applications", *Developments in the Built Environment*, 1, 100004, 2020. <https://doi.org/10.1016/j.dibe.2019.100004>
- [2] Arciszewska-Kędzior, A., Kunecký, J., Hasníková, H., Sebera, V. "Lapped Scarf Joint with Inclined Faces and Wooden Dowels: Experimental and Numerical Analysis", *Engineering Structures*, 94, pp. 1–8, 2015. <https://doi.org/10.1016/j.engstruct.2015.03.036>
- [3] Johansen, K. W. "Theory of timber connections", *International Association for Bridge and Structural Engineering*, 9, pp. 249–262, 1949. <https://doi.org/10.5169/seals-9703>
- [4] CEN "EN 1995-1-1:2004 Eurocode 5. (E) Design of Timber Structures", European Committee for Standardization, Brussels, Belgium, 2004.
- [5] Dorn, M., de Borst, K., Eberhardsteiner, J. "Experiments on Dowel-Type Timber Connections", *Engineering Structures*, 47, pp. 67–80, 2013. <https://doi.org/10.1016/j.engstruct.2012.09.010>
- [6] Xu, B. H., Taazount, M., Bouchaïr, A., Racher, P. "Numerical 3D Finite Element Modelling and Experimental Tests for Dowel-Type Timber Joints", *Construction and Building Materials*, 23(9), pp. 3043–3052, 2009. <https://doi.org/10.1016/j.conbuildmat.2009.04.006>
- [7] Xu, B. H., Jiao, S. Y., Wang, B. L., Bouchaïr, A. "Mechanical Performance of Timber-to-Timber Joints with Densified Wood Dowels", *Journal of Structural Engineering*, 148(4), 2022. [https://doi.org/10.1061/\(ASCE\)ST.1943-541X.0003317](https://doi.org/10.1061/(ASCE)ST.1943-541X.0003317)
- [8] Conway, M., Mehra, S., Harte, A. M., O’Ceallaigh, C. "Densified Wood Dowel Reinforcement of Timber Perpendicular to the Grain: A Pilot Study", *Journal of Structural Integrity and Maintenance*, 6(3), pp. 177–186, 2021. <https://doi.org/10.1080/24705314.2021.1906090>
- [9] Riggio, M., Sandak, J., Sandak, A. "Densified Wooden Nails for New Timber Assemblies and Restoration Works: A Pilot Research", *Construction and Building Materials*, 102, pp. 1084–1092, 2016. <https://doi.org/10.1016/j.conbuildmat.2015.06.045>
- [10] Grönquist, P., Schnider, T., Thoma, A., Gramazio, F., Kohler, M., Burgert, I., Rüggeberg, M. "Investigations on Densified Beech Wood for Application as a Swelling Dowel in Timber Joints", *Holzforschung*, 73(6), pp. 559–568, 2019. <https://doi.org/10.1515/hf-2018-0106>
- [11] Feio, A. O., Lourenço, P. B., Machado, J. S. "Testing and Modeling of a Traditional Timber Mortise and Tenon Joint", *Materials and Structures*, 47(1–2), pp. 213–225, 2014. <https://doi.org/10.1617/s11527-013-0056-y>
- [12] Koch, H., Eisenhut, L., Seim, W. "Multi-Mode Failure of Form-Fitting Timber Connections – Experimental and Numerical Studies on the Tapered Tenon Joint", *Engineering Structures*, 48, pp. 727–738, 2013. <https://doi.org/10.1016/j.engstruct.2012.12.002>
- [13] Caldeira, T. V. P., Dourado, N., De Jesus, A. M. P., De Moura, M. F. S. F., Morais, J. J. L. "Quasi-Static Behavior of Moment-Carrying Steel–Wood Doweled Joints", *Construction and Building Materials*, 53, pp. 439–447, 2014. <https://doi.org/10.1016/j.conbuildmat.2013.11.078>
- [14] Santos, C., De Jesus, A. M. P., and Morais, J. J. L. "Mechanical Behaviour of Wood T-Joints. Experimental and Numerical Investigation", *Fracture and Structural Integrity*, 9(31), pp. 23–37, 2014. <https://doi.org/10.3221/IGF-ESIS.31.03>
- [15] Schoenmakers, J. C. M., Jorissen, A. J. M. "Failure Mechanisms of Dowel-Type Fastener Connections Perpendicular to Grain", *Engineering Structures*, 33, pp. 3054–3063, 2011. <https://doi.org/10.1016/j.engstruct.2011.05.018>
- [16] Shanks, J. D., Chang, W.-S., Komatsu, K. "Experimental Study on Mechanical Performance of All-Softwood Pegged Mortise and Tenon Connections", *Biosystems Engineering*, 100, pp. 562–570, 2008. <https://doi.org/10.1016/j.biosystemseng.2008.03.012>

- [17] Guan, Z., Komatsu, K., Jung, K., Kitamori, A. "Structural Characteristics of Beam–Column Connections Using Compressed Wood Dowels and Plates", In: 11th World Conference on Timber Engineering 2010 (WCTE 2010), Trentino, Italy, 2010, pp. 2749–2756. ISBN 9781622761753
- [18] Daudeville, L., Davenne, L., Yasumura, M. "Prediction of the Load Carrying Capacity of Bolted Timber Joints", *Wood Science and Technology*, 33(1), pp. 15–29, 1999.  
<https://doi.org/10.1007/s002260050095>
- [19] Saad, K., Lengyel, A. "A Parametric Investigation of the Influence of Knots on the Flexural Behavior of Timber Beams", *Periodica Polytechnica Civil Engineering*, 67(1), pp. 261–271, 2023.  
<https://doi.org/10.3311/PPci.21360>
- [20] Milić, M., Vacev, T., Petronijević, P., Nešović, I., Zorić, A., Paunović, S., Matejević Nikolić, B. "Experimental Research and FE Model of a Bolted Steel-CLT Composite Connection", *Periodica Polytechnica Civil Engineering*, 68(1), pp. 8–22, 2024.  
<https://doi.org/10.3311/PPci.22752>
- [21] Lengyel, A., Saad, K. "Experimental and Numerical Analysis of Structural Integrity and Fibre Reinforcement of Aged Timber Beams Containing Knots and Checks", *Engineering Structures*, 337, 120446, 2025.  
<https://doi.org/10.1016/j.engstruct.2025.120446>
- [22] Hill, R. "A Theory of the Yielding and Plastic Flow of Anisotropic Metals", *Proceedings of the Royal Society of London. Series A. Mathematical and Physical Sciences*, 193(1033), pp. 281–297, 1948.  
<https://doi.org/10.1098/rspa.1948.0045>
- [23] Hoffman, O. "The Brittle Strength of Orthotropic Materials", *Journal of Composite Materials*, 1(2), pp. 200–206, 1967.  
<https://doi.org/10.1177/002199836700100210>
- [24] Tabiei, A., Wu, J. "Three-Dimensional Nonlinear Orthotropic Finite Element Material Model for Wood", *Composite Structures*, 50(2), pp. 143–149, 2000.  
[https://doi.org/10.1016/S0263-8223\(00\)00089-1](https://doi.org/10.1016/S0263-8223(00)00089-1)
- [25] Tagarielli, V. L., Deshpande, V. S., Fleck, N. A., Chen, C. "A Constitutive Model for Transversely Isotropic Foams, and Its Application to the Indentation of Balsa Wood", *International Journal of Mechanical Sciences*, 47(4–5), pp. 666–686, 2005  
<https://doi.org/10.1016/j.ijmecsci.2004.11.010>
- [26] Schellekens, J. C. J., de Borst, R. "The Use of the Hoffman Yield Criterion in Finite Element Analysis of Anisotropic Composites", *Computers & Structures*, 37(6), pp. 1087–1096, 1990.  
[https://doi.org/10.1016/0045-7949\(90\)90020-3](https://doi.org/10.1016/0045-7949(90)90020-3)
- [27] Reiterer, A., Stanzl-Tschegg, S. E. "Compressive Behaviour of Softwood under Uniaxial Loading at Different Orientations to the Grain", *Mechanics of Materials*, 33(12), pp. 705–715, 2001.  
[https://doi.org/10.1016/S0167-6636\(01\)00086-2](https://doi.org/10.1016/S0167-6636(01)00086-2)
- [28] Tran, T. T., Dao, N. T. "Development of a Hybrid Elasto–Plastic–Damage Material Model for the Analysis of Adhesive-Free Lapped Scarf Timber Joints", *Mechanics Based Design of Structures and Machines*, 54(1), 2632701, 2026.  
<https://doi.org/10.1080/15397734.2026.2632701>